Pseudospherical integration scheme for electronic-structure calculations

F. W. Averill* and G. S. Painter
Metals and Ceramics Division, Oak Ridge National Laboratory, Oak Ridge, Tennessee 37831
(Received 18 July 1988)

Contemporary electronic-structure methods avoid shape approximations but in doing so encounter the difficult problem of integral evaluation over complicated interstitial volumes. In this paper, we present a simple and efficient technique for applying rapidly convergent Gaussian product formulas to general interstitial regions. Like the recent methods of Boerrigter, te Velde, and Baerends, it is based upon partitioning space into Voronoi cells and atomic spheres. In the present work, introduction of a general pseudospherical local-coordinate system unifies the integration procedures and effects a simplified approach. A systematic procedure is derived for determining the number of Gaussian points required for a specified level of numerical precision.

I. INTRODUCTION

A common problem encountered in molecular and solid-state electronic-structure calculations is the need to evaluate three-dimensional multicenter integrals without imposing shape approximations on the charge density or potential. In the local-spin-density approximation,[1] the exchange-correlation potential is not a linear functional of the charge density, and matrix elements of the potential must be evaluated numerically. Matrix elements of the electron-electron potential can be determined analytically in some basis sets, but even for these integrals numerical methods have sometimes proven to be more efficient.[2] Many workers have discovered that a combination of numerical and analytical algorithms seems to offer the most effective approach.[3]

One approach to the multicenter integration problem involves partitioning the space of a molecule or solid into Wigner-Seitz–type cells, called Voronoi polyhedra, around each atom. The Voronoi polyhedron about a particular atom is constructed by enclosing the atom with the closest planes that are perpendicular bisectors of lines drawn from the atom to the other atoms in the solid or molecule. Becke[4] has proposed an interesting scheme for multicenter numerical integration which is based on such partitioning, but with modifications to reduce the multicenter integration to a sum of single-center integrals. The present work is more in the spirit of that of Boerrigter *et al.*,[5] who find it advantageous to treat singularities at the nuclei by surrounding each atom in the Voronoi cell by a sphere in which integration in spherical coordinates can be carried out. Integration over the Voronoi cell is then composed of two parts: (1) integration within the atom sphere, and (2) integration over the interstitial region (i.e., the region outside the sphere but inside the cell). The integration inside the atomic sphere is easily handled using product Gaussian formulas[6,7] over spherical coordinates, but because of the nonspherical shape of the Voronoi-cell faces, the integration over the interstitial region is more problematic.

In order to deal with the interstitial region, Boerrigter *et al.* suggest that the Voronoi cell be filled by polyhedra in such a manner that the base of each polyhedron is a planar region on the surface of the cell and the major vertex of the polyhedron is at the center of the atom. This polyhedron will have $n+1$ planar faces, where n is the number of sides of its base. The faces of a Voronoi cell will be planar polygons with possibly differing numbers of sides, but each face can always be divided into a connected set of triangles and quadrilaterals. In principle, triangles alone would be sufficient, but our experience has shown that this is not always the best choice. Division into quadrilaterals is found to offer added flexibility to the cell face partitioning procedure.

In the development presented here, each polyhedron inside the cell will be chosen to have either four faces (for a triangular base) or five faces (for a quadrilateral base). We will refer to such polyhedra as *generalized cones* or just simply cones. However, it must be understood that unlike a regular cone or a regular pyramid, the vertex of a generalized cone will not necessarily be located directly over the center of its base, i.e., a generalized cone may be skewed. We note that this definition of the generalized cone is somewhat different from that of Refs. 5 and 6.

If the portion of a cone inside the atomic sphere is eliminated, the remaining part of the cone lies entirely in the interstitial region of the Voronoi cell. In fact, the set of all such truncated cones will form a partition of the interstitial volume of the Voronoi cell. An integral over the interstitial volume alone can consequently be written as a sum of integrals over truncated cones. In their paper, Boerrigter *et al.*[5] point out that the integral of the function $f(x,y,z)$ over the volume of the truncated cone can be written in spherical coordinates centered at the atom as

$$\int\int\int f(x,y,z)\,dx\,dy\,dz = \int_{\Omega_0}\left[\int_{r_s}^{r_0(\Omega)} f(r,\Omega)r^2\,dr\right]d\Omega\ , \quad (1)$$

where r_s is the atom sphere radius, $r_0(\Omega)$ is the radial distance from the origin to the base of the cone at angle Ω, and Ω_0 is the set of angles which sweeps over the base of the cone.

In Ref. 5 only the case of a cone with a quadrilateral base is treated by use of Eq. (1). The case of a cone with a triangular base is also treated, but by a different approach using a Cartesian-coordinate system. In the present work, we present a unified development of integration over cones with triangular and quadrilateral bases. We anticipate that this unification of the two kinds of cones, along with the computational details on grid-point generation that we present, will simplify the computational implementation of three-dimensional Gauss integration procedures for interstitial volumes.

II. PSEUDOSPHERICAL COORDINATES IN GENERALIZED CONES

The starting point of our development is to consider integration of a function $f(x,y,z)$ over the volume of a generalized cone with an arbitrary surface (B) as its base (Fig. 1). For every point P_0 on B, we define an ordered pair of coordinates (s,t) which is local to that surface. We also assume that Cartesian coordinates of points on the surface are known functions of the variables s and t:

$$x_0=x_0(s,t),\quad y_0=y_0(s,t),\quad z_0=z_0(s,t)\ . \tag{2}$$

The Cartesian coordinates of an arbitrary point P defined by vector $\mathbf{r}$ inside the cone (Fig. 1) can be given in terms of the direction cosines of the point as

$$x=r\cos\theta_x,\quad y=r\cos\theta_y,\quad z=r\cos\theta_z\ , \tag{3}$$

where

$$\cos\theta_x=\frac{x_0}{r_0},\quad \cos\theta_y=\frac{y_0}{r_0},\quad \cos\theta_z=\frac{z_0}{r_0}\ , \tag{4}$$

$$r_0=(x_0^2+y_0^2+z_0^2)^{1/2}\ . \tag{5}$$

The vector $\mathbf{r}_0$ is determined by the extension of $\mathbf{r}$ to the surface B (Fig. 1) at $P_0(s,t)$.

It is then a straightforward exercise in vector calculus

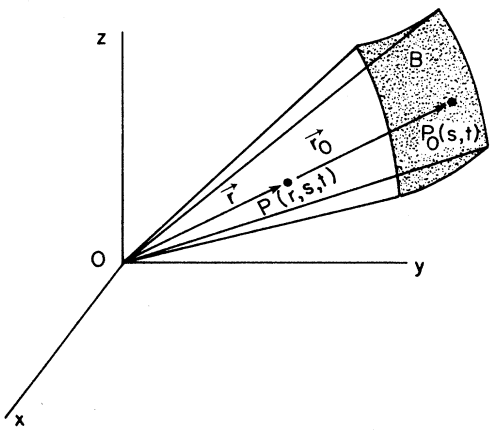

FIG. 1. Pseudospherical coordinate system with local surface variables s and t. An arbitrary point, P, in the space can be specified by its distance from the origin (r) and the local surface variables (s,t) determined by the intersection of $\mathbf{r}_0$ (the extension of $\mathbf{r}$ to the surface B) at the point $P_0(s,t)$.

to show that the Jacobian for the volume integration over the variables (r,s,t) can be written as

$$J=r^2\left|\hat{\mathbf{r}}_0\cdot\left[\frac{\partial\hat{\mathbf{r}}_0}{\partial s}\times\frac{\partial\hat{\mathbf{r}}_0}{\partial t}\right]\right|\ , \tag{6}$$

where $\hat{\mathbf{r}}_0$ is the unit vector, $\hat{\mathbf{r}}_0=\mathbf{r}_0/|\mathbf{r}_0|$. An important aspect displayed by the Jacobian, Eq. (6), is that the unit vector does not depend on r. All the r dependence of J is contained in r^2 and all the dependence of J on the basal parameters s and t is contained in the triple product function of s and t,

$$v(s,t)=\left|\hat{\mathbf{r}}_0\cdot\left[\frac{\partial\hat{\mathbf{r}}_0}{\partial s}\times\frac{\partial\hat{\mathbf{r}}_0}{\partial t}\right]\right|\ . \tag{7}$$

For the sake of geometric interpretation, it can be shown that the vectors $\partial\hat{\mathbf{r}}_0/\partial s$ and $\partial\hat{\mathbf{r}}_0/\partial t$ are vectors tangential to the surface B at the point $P_0(s,t)$. The triple product $v(s,t)$ is the volume of a parallelepiped with sides formed by the vectors $\hat{\mathbf{r}}_0$, $\partial\hat{\mathbf{r}}_0/\partial s$, and $\partial\hat{\mathbf{r}}_0/\partial t$.

Equation (6) is quite general and is appropriate to any surface which has the properties we have described. For instance, by letting s and t be the standard spherical coordinates θ,ϕ of points on the surface of a sphere, one obtains the familiar Jacobian, $J=r^2\sin(\theta)$. It is now perhaps clear to the reader why, for an arbitrary surface B, we refer to the coordinates (r,s,t) as pseudospherical. The local coordinates (s,t) specify points on a surface B and define a direction in space in much the same way as the spherical coordinates (θ,ϕ).

In this work we focus on planar surfaces, and in the following we assume that the reference surface is of this type. We also assume that the plane of the surface is perpendicular to the x axis. This assumption is not a restriction since for an arbitrary plane the Cartesian-coordinate system may be rotated so that the x axis is aligned along the perpendicular from the origin to the plane. Since the Jacobian depends only on the local coordinates (s,t) and the radial variable r, it will be independent of the rotation. Once the vector $\mathbf{r}_0(s,t)$ and its derivatives $\partial\mathbf{r}_0/\partial s$ and $\partial\mathbf{r}_0/\partial t$ are specified as functions of s and t, it is then a simple matter to evaluate the Jacobian J for an arbitrary point $P(r,s,t)$ using Eq. (6). In the next section we will define local coordinate systems (s,t) for quadrilateral and triangular surfaces which are particularly well adapted to the use of product Gaussian formulas for numerical integration.

III. CONES WITH QUADRILATERAL AND TRIANGULAR BASES

We begin our discussion by considering some possible choices for the local coordinates (s,t). In Fig. 2 the s and t coordinates for integration points on the surface of planar quadrilateral and triangular regions in the rotated coordinate system are defined. The quadrilateral and triangular regions are the type surfaces that form bases of the cones (Fig. 1) we consider. Since the plane of each base is chosen perpendicular to the x axis, the x coordinate of points on each polygon will be a constant, and the derivatives $\partial x_0/\partial s$ and $\partial x_0/\partial t$ will be zero. One has to-

tal freedom in the choice of the local variables (s,t), but it is best to choose a parametrization of y_0 and z_0 in terms of s and t which facilitates specification of points on the polygonal surface.

One suitable choice for the quadrilateral in Fig. 2(a) is

$$y_0=y_1+(y_4-y_1)t+[(y_2-y_1)+(y_3+y_1-y_4-y_2)t]s \tag{8}$$

and

$$z_0=z_1+(z_4-z_1)t+[(z_2-z_1)+(z_3+z_1-z_4-z_2)t]s\ , \tag{9}$$

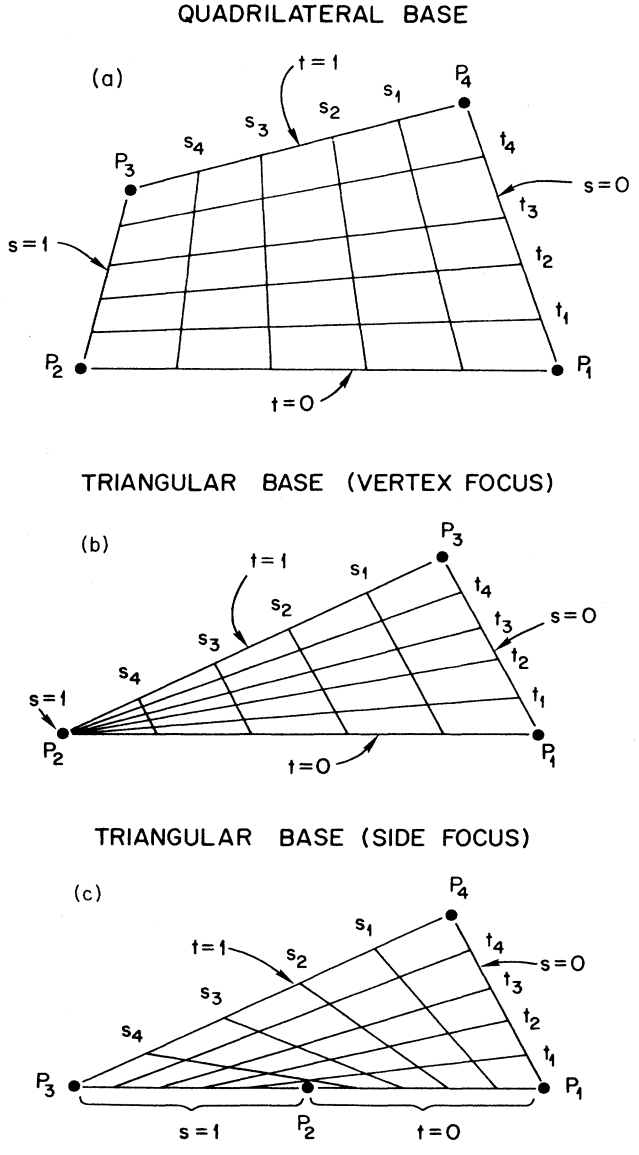

FIG. 2. (a) Quadrilateral and (b) and (c) triangular bases for generalized cones. Constant s and constant t contours are generated by (a) Eqs. (8) and (9) for a quadrilateral, (b) Eqs. (10) and (11) for a triangle, and (c) Eqs. (8) and (9) applied to a triangle with an artificial vertex (P_2) introduced on the largest side.

where (y_i,z_i) denote the yz coordinates of vertex "i." In this scheme the contours of constant s will be straight lines in the quadrilateral which approach the side P_1P_4 as $s\rightarrow 0$ and which approach side P_2P_3 as $s\rightarrow 1$. Similarly, the contours of constant t will be lines approaching P_1P_2 as $t\rightarrow 0$ and approaching P_3P_4 as $t\rightarrow 1$. As s and t range between zero and one, the points (y_0,z_0) will be on or inside the quadrilateral.

A comparable parametrization can be carried out for the triangle in Fig. 2(b) using *area coordinates*.[7,8] Here

$$y_0=y_1+(y_2-y_1)s+(y_3-y_1)t(1-s) \tag{10}$$

and

$$z_0=z_1+(z_2-z_1)s+(z_3-z_1)t(1-s)\ . \tag{11}$$

Unfortunately, this choice for y_0 and z_0 has the asymmetric feature that all contours of constant t converge at P_2. However, we have used integration grids generated by Eqs. (10) and (11) and have found them to be satisfactory, although the efficiency of the grid (i.e., the total number of points necessary to obtain a given level of numerical accuracy) may depend upon the way the vertices of the triangle are chosen. In particular, if the integrand is large and changing rapidly in the direction of a particular vertex, it is logical to choose that as the vertex where the highest density of points in the integration grid will occur [e.g., P_2 in Fig. 2(b)].

An alternative way to handle the parametrization of the triangle is to introduce an artificial vertex in the middle of one of the sides of the triangle and to treat the triangle as a pseudoquadrilateral with Eqs. (8) and (9). The result of this approach [Fig. 2(c)] is a concentration of points about the artificial vertex. Again, as was the case with the first parametrization of the triangle [Eqs. (10) and (11)], there may be circumstances under which this clustering of points can be used to advantage.

For grids with particular numbers of points, there are so-called symmetric point distributions for triangles available in the literature.[6,8,9] Unfortunately, the symmetric grids that presently exist are not generally dense enough to provide sufficient accuracy for electronic-structure calculations. In any case, the problem of the truncated cone with a triangular base can be successfully dealt with using either Eqs. (8) and (9) or Eqs. (10) and (11).

The integral of a function $f(x,y,z)$ over the volume of a truncated cone, with either a quadrilateral or triangular base, can be written as

$$\int_{\Omega_0}\left[\int_{r_s}^{r_0(\Omega)} f(r,\Omega)r^2\,dr\right]d\Omega = \int_0^1\int_0^1 v(s,t)\left[\int_{r_s}^{r_0(s,t)} f(r,s,t)r^2\,dr\right]dt\,ds\ . \tag{12}$$

A product Gaussian formula can be used directly to evaluate the integrals over the variables s and t, and the integral over r, which depends on s and t, can also be treated by Gaussian quadrature using the method of iterated integrals.[6]

IV. COMPUTATIONAL DETAILS AND EXAMPLE

In this section we look at some of the computational details associated with the method of truncated cones. As a specific system for illustration, we chose a cluster of six nickel atoms arranged at the vertices of a regular octahedron, $(\pm d,0,0)$, $(0,\pm d,0)$, and $(0,0,\pm d)$. Results from a study of this system using an earlier three-dimensional Gaussian integration scheme have been published elsewhere,[10] and we focus here only on the problem of generating a numerical integration grid for the interstitial region.

A. Symmetry wedges

The first step in setting up the point grid is to partition the space around the atoms in an optimum way. In the preceding sections we have discussed the partitioning of the volume around the atoms in a molecule or a solid into Voronoi cells about each atom. It should be understood, however, that the use of Voronoi cells is only one way to fill the space with polyhedra. The method of truncated cones is independent of the details of the specific partitioning. Since most of the molecular integrals of interest need only be performed over the smallest volume which can generate the space by symmetry operations, the partitioning should be carried out so as to take advantage of the spatial symmetry of the cluster.

In the Ni_6 cluster, we have chosen a wedge which projects out from the center of the octahedron (Fig. 3) which encompasses $\frac{1}{48}$ of all space. The edges of the wedge are along the (1,0,0), (1,1,0), and (1,1,1) directions. Although molecular integrals formally require integration over all space, in practice the integration space can be terminated at some appropriate finite distance. We have chosen to enclose the $\frac{1}{48}$ wedge with a triangular face whose vertices are (in a.u.) at (16,0,0), (8,8,0), and (8,8,8). It should be mentioned that the coordinates that are given for this triangle and those that will be given later for the truncated cones and atom positions are for a *reference space.* The points and atom positions in this reference space are then linearly scaled to produce isotropic expansions and contractions of the cluster. In other clusters with more than one inequivalent atom, it may be necessary to introduce more than one scale factor in order to allow the cones associated with the different types of atoms to move independently of one another. In the present case, the finite $\frac{1}{48}$ wedge is a four-sided polyhedron (Fig. 3) with vertices (in a.u.) at (0,0,0), (16,0,0), (8,8,0), and (8,8,8) with the nickel atom located at (2.6,0,0).

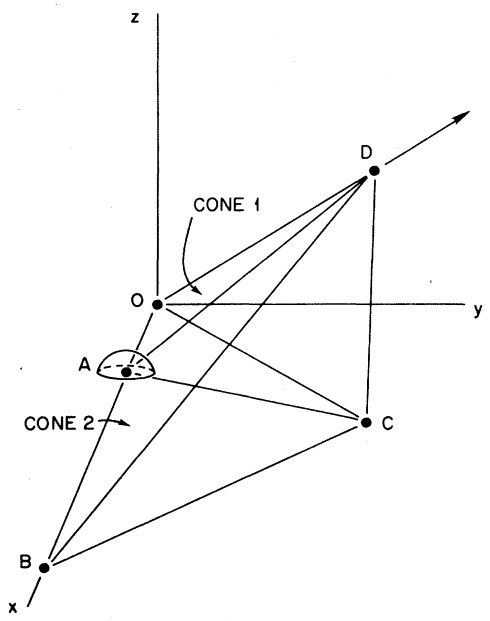

FIG. 3. Irreducible $\frac{1}{48}$ symmetry wedge defined for numerical integration in the interstitial region of an octahedral Ni_6 cluster. The wedge can be partitioned into a minimum of two cones with vertices O, A, C, D for cone 1 and vertices A, B, C, D from cone 2. The atom in the wedge is located at A. The Cartesian coordinates of the vertices are, in a.u., O(0,0,0), A(2.6,0,0), B(16,0,0), C(8,8,0), and D(8,8,8).

B. Choice of cones

The second step in the point-grid construction is to fill the $\frac{1}{48}$ wedge with cones, each with its major vertex at the atom site. In the present case, there is a minimum number of two such cones which fill the space. These two cones have triangular bases on sides of the $\frac{1}{48}$ wedge with base vertices (0,0,0), (8,8,0), and (8,8,8) for one cone and (8,8,8), (8,8,0), and (16,0,0) for the other. Experience has shown that more efficient grids (i.e., grids with fewer points for the same level of numerical accuracy) are often obtained by using more than the minimum number of cones.

This process of partitioning the $\frac{1}{48}$ wedge into cones in a more or less optimal way requires some trial and error, but the basic idea is to heavily partition the regions of space where the integrands are large and rapidly changing and to sparingly partition regions where integrands are small and smooth. Obviously, it is impractical to use a different grid for each of the many different integrands that occur in a large electronic-structure calculation. One must obtain one grid which is likely to be satisfactory for all the required molecular integrals. What is needed is a representative integrand which (1) has the gross features of all molecular integrands, i.e., is large and rapidly changing near the atoms and is small and slowly varying at large distances; (2) is easily and efficiently evaluated on the computer; and (3) provides an accurate check, i.e., the integral value is known. One can then proceed to optimize the point grid for this representative integrand in the expectation that the same mesh will be efficient and accurate for each of the molecular integrals.

In earlier augmented-Gaussian-basis calculations,[2] only integrals over the exchange-correlation and Coulomb potentials, each multiplied by a pair of basis functions, are evaluated numerically. We have found that a point grid optimized to integrate the total charge density of a particular system efficiently also evaluates general molecular integrands quite satisfactorily. We have, as a consequence, chosen the total charge density as

TABLE I. Gaussian product grid for the two-cone partitioning of the interstitial region of the $\frac{1}{48}$ wedge in the Ni_6 cluster (see Fig. 3). The atom sphere radius was chosen so that the spheres of nearest neighbors touch but do not overlap. In cone 1, the base *OCD* was parametrized so that the edge *CD* corresponds to $s=0$ and the vertex *O* to $s=1$ [see Figs. 2(b) and 3]. For cone 2, $s=0$ at edge *BD* and $s=1$ at *C*. The exact interstitial charge of the model superimposed atom charge density over the entire cluster is 6.294 661 9.

Cone number	Number of r points	Number of s points	Number of t points	Total number of points	Charge
1	20	40	7	5600	4.428 040 7
2	20	7	5	700	1.866 616 9
			Total	6300	6.294 657 6

our representative integrand. The total charge integral has the added advantage that its value is exactly known, and with Gaussian basis sets partial charge densities (e.g., the interstitial charge) can also be evaluated exactly using analytic Gaussian-function integral algorithms. The error of the numerical integral of the charge density can then be precisely determined.

C. Grid-point selection

The third step of the grid construction is to optimize the number of Gaussian integration points in each cone necessary to obtain a specified level of accuracy in the integral of the representative integrand over the cone. The point grid in each cone is optimized independently. Also within a given cone, integration in each of the three variables is successively optimized independent of the other two. The number of Gaussian points in each of the three coordination variables is incremented in turn until the absolute change in the integral between increments is less than some specified value. We have found, for example, that an accuracy of 0.000 002 in each of the three integration directions within a cone will generally give a total charge integral over all cones with an error no larger than about 0.000 05. This accuracy in the charge density, in turn, ensures that the total energy of the final self-consistent calculation will have a numerical error no greater than about 0.05 eV. Higher precision requires commensurately finer integration grids.

Of course, the point grids of the three coordinates within a cone are not truly independent of one another and some "cycling" in the optimization process may be necessary before the point grid becomes "self-consistent." By self-consistent we mean that if the optimization process is begun with that point grid, the outcome of the process will be the same point grid. Usually only a single cycle is necessary.

The point-grid–optimization process described above is carried out on the computer. In the early stages of the process, we have found it efficient to use a molecular charge density approximated by a superposition of atom charge densities as the representative integrand. These atom densities are given in terms of analytic Gaussian functions and can be evaluated very quickly on the computer. This superimposed charge density, however, is typically more spherically symmetric about the atom sites than the density from molecular wave functions. Therefore, in the final stages of the optimization in the "angular" directions of s and t, the superimposed atom density is replaced by a more realistic calculated molecular charge density.

D. Numerical example: Ni_6

Tables I, II, and III illustrate successive tests of different partitions of the interstitial region of the $\frac{1}{48}$ wedge in the Ni_6 cluster.

For the result of Table I, the minimum number of two cones was used (see Fig. 3). The point-optimization program was started with only five points in each of the three dimensions in each of the two cones. The program proceeds to increase (and decrease) the number of points in each of the three dimensions in each cone until the absolute change in the superimposed atom charge integral between increments is $\leq 0.000\,002$. Although Gaussian

TABLE II. Results for interstitial charge integral with five-cone partitioning of $\frac{1}{48}$ wedge interstitial region. For cone labels, see Fig. 4 and text. Exact charge integral value is 6.294 661 9.

Cone no.	No. of r points	No. of s points	No. of t points	Total no. of points	Total points	Charge	Total charges
1a	3	7	5	105		0.399 408 1	
1b	3	5	7	105		0.766 910 5	
1c	8	8	5	320		2.329 098 1	
1d	20	7	5	700	1230	0.932 621 4	4.428 038 1
2	20	7	5	700	700	1.866 616 9	1.866 616 9
				Total	1930		6.294 655 0

TABLE III. Results for interstitial charge integral using eight-cone partitioning of $\frac{1}{48}$ wedge. See Fig. 4 and text for cone definitions. Exact integral value is 6.294 661 9.

Cone no.	No. of r points	No. of s points	No. of t points	Total no. of points	Total points	Charge	Total charges
1a	3	6	5	90		0.399 408 2	
1b	3	5	6	90		0.766 910 6	
1c	7	7	5	245		2.329 099 8	
1d.1	5	5	5	125		0.704 539 1	
1d.2	8	6	5	240	790	0.228 081 9	4.428 039 6
2.1	5	6	5	150		1.455 725 7	
2.2	9	6	4	216	366	0.410 891 5	1.866 617 2
				Total	1156		6.294 656 8

grids of 40 points are readily handled, as a rule of thumb, we usually partition space until the number of points in any dimension within a cone is less than about 10. The excessive number of points (Table I) required in the s and r channels of the first cone and the r channel of the second cone is indicative of the need to further partition the cones in those variables.

Figure 4 shows how the first cone (of Fig. 3) can be partitioned in the s direction and Table II gives the point-optimization outcome for that partitioning. It can be seen from Tables I and II that the total number of points required in the first cone has been reduced from 5600 to 1230.

Consider now the partitioning of cones 1d and 2 in the r direction (where r extends from the atomic site). The large number of r points in cones 1d and 2 is due to the fact that these cones extend out from the atom sphere to the practical infinity of the outer wedge surface. Experience has shown that a satisfactory result can be obtained by partitioning out the region close to the atom where the charge density is particularly large. We therefore partition cones 1d and 2 into cones 1d.1 and 2.1, respectively (not shown), which project out from the atom sphere surface ($r_s = 1.8384$) to a radius of 3.0 and cones 1d.2 and 2.2 which proceed from $r = 3.0$ out to the $\frac{1}{48}$ wedge surface.[11]

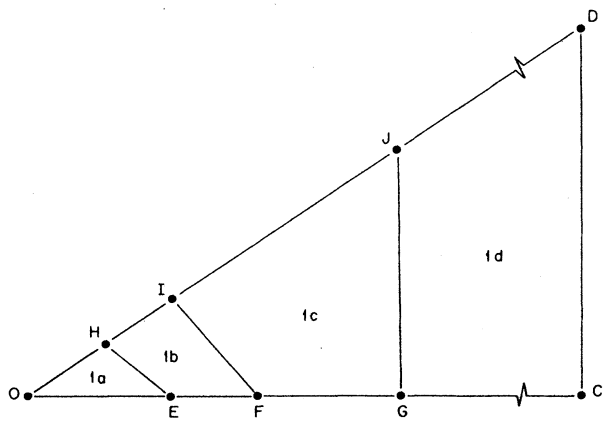

FIG. 4. Partitions of the (110) surface of cone 1 into the four cones 1a, 1b, 1c, and 1d. The Cartesian coordinates of the vertices of these cones are, in a.u., O(0,0,0), E(1.45,14.5,0), F(2.44,24.44,0), G(4,4,0), C(8,8,0), D(8,8,8), J(4,4,4), I(1.53,1.53,1.53), and H(0.82,0.82,0.82).

Table III is the optimized point grid for the final partitioning of the $\frac{1}{48}$ wedge. This table is the result of iterating once producing a self-consistent grid. It can be seen that the cycling has had the effect of reducing the number of points in cones 1a, 1b, and 1c. At this stage in the point-generation process the superimposed atom charge density would normally be replaced by a real molecular charge density and the last stage of "fine tuning" the point grid would be accomplished. Typically, such fine tuning only slightly increases the number of s or t points in several of the cones.

It should also be pointed out that the point grids of triangular cones used in this partitioning were generated from Eqs. (10) and (11). We have at other times used the quadrilateral formulas [Eqs. (8) and (9)] for the triangular cones without much change from the results given in the tables here. Furthermore, the results presented in the tables were obtained for a specific scale factor (1.211 54) and would be expected to vary somewhat as the scale factor is changed to describe different cluster geometries. It has been our experience that if the scale factor is changed by more than about 20–30 %, the point grid should be reoptimized in order to maintain a consistent level of numerical accuracy.

V. CONCLUSION

In the original form of the augmented-Gaussian-basis technique developed by the present authors,[2] integrations over the interstitial region were performed by first integrating with Gaussian quadrature over a set of wedges chosen to divide up the $\frac{1}{48}$ wedge and then subtracting out the integrals over the atom spheres. Since the integrals over the spheres were added in and then subtracted out, the integrand in the spheres could be chosen to be any function which joins smoothly to the integrand in the interstitial region. This integration technique proved quite efficient in practice and was used in a number of different studies.[2,10,12–14]

The new interstitial integration scheme described in this paper has now been incorporated into our computer

codes and requires less computer time while being simpler to apply. In the previous scheme it was necessary to partition up the entire $\frac{1}{48}$ wedge, whereas with the present technique using truncated cones, partitioning applies only to the interstitial region. The integration methods presented here are quite general and should be of value in evaluation of similar kinds of three-dimensional integrals. Although the technique was developed for applications within the local-spin-density method, there is no reason why the numerical procedures described here could not be implemented in other types of electronic-structure calculations as well.

ACKNOWLEDGMENTS

This research was sponsored by the Division of Materials Sciences, U.S. Department of Energy, under Contract No. DE-AC05-84OR21400 with Martin Marietta Energy Systems, Inc.

APPENDIX: TRANSFORMATION OF POINTS FROM THE ROTATED COORDINATE SYSTEM

In order to calculate the Gaussian integration points and weights from Eqs. (8)–(11), it is convenient to rotate the x axis so that it is perpendicular to the plane of the base of the truncated cone. The points so generated must then be transformed back into the original molecular coordinate system before they are actually used in the calculation.

The mathematical development for carrying out this transformation can be found in most texts[15] dealing with three-dimensional vector spaces. For the sake of completeness, a brief description of the process is given below.

A vector normal to the plane of three noncollinear vertices $P_1(x_1,y_1,z_1)$, $P_2(x_2,y_2,z_2)$, and $P_3(x_3,y_3,z_3)$ of a planar polygon can be computed as the cross product of the two vectors (P_1,P_2) and (P_1,P_3) as

$$\mathbf{n}=(P_1,P_2)\times(P_1,P_3)=(a,b,c)\ , \tag{A1}$$

where the x,y,z coordinate components (a,b,c) can be determined from the Cartesian coordinate of the points P_1, P_2, and P_3.

A perpendicular from the origin to the plane of the polygon intersects the plane at the point (ta,tb,tc) where

$$t+\frac{ax_1+by_1+cz_1}{a^2+b^2+c^2}\ . \tag{A2}$$

The vector

$$\hat{\mathbf{i}}_A=\frac{t(a,b,c)}{|t|(a^2+b^2+c^2)^{1/2}}\ , \tag{A3}$$

becomes the x-coordinate unit vector for the rotated coordinated system. There is considerable freedom as to how the y and z axes for the rotated coordinate system are selected, but we have arbitrarily chosen to let the vector drawn from the first vertex to the second be the direction of the rotated y axis. Then,

$$\hat{\mathbf{j}}_A=\frac{(P_1,P_2)}{|P_1,P_2|}\ , \tag{A4}$$

and to ensure a right-handed coordinate system,

$$\hat{\mathbf{k}}_A=\hat{\mathbf{i}}_A\times\hat{\mathbf{j}}_A\ . \tag{A5}$$

Finally, the elements of the matrix which transforms points in the rotated system back into the original molecular coordinate system are given by the components of the unit vectors $\hat{\mathbf{i}}_A$, $\hat{\mathbf{j}}_A$, and $\hat{\mathbf{k}}_A$ in the original coordinate system.

---

*Permanent address: Judson College, Elgin, Illinois 60123.

[1]W. Kohn and L. J. Sham, Phys. Rev. **140**, A1133 (1965).

[2]G. S. Painter and F. W. Averill, Phys. Rev. B **28**, 5536 (1983).

[3]For a recent review of local-spin-density methods, see D. R. Salahub, in *Ab Initio Methods in Quantum Chemistry II*, edited by K. P. Lawley (Wiley, New York, 1987).

[4]A. D. Becke, J. Chem. Phys. **88**, 2547 (1988).

[5]P. M. Boerrigter, G. te Velde, and E. J. Baerends, Int. J. Quantum Chem. **33**, 87 (1988).

[6]A. H. Stroud, *Approximate Calculations of Multiple Integrals* (Prentice-Hall, Englewood Cliffs, NJ, 1971).

[7]A. H. Stroud and D. Secrest, *Gaussian Quadrature Formulas* (Prentice-Hall, Englewood Cliffs, NJ, 1966).

[8]J. E. Akin, *Application and Implementation of Finite Element Methods* (Academic, New York, 1982).

[9]P. C. Hammer, O. J. Marlowe, and A. H. Stroud, Math. Tables Other Aids Comput. **10**, 130 (1956).

[10]G. S. Painter and F. W. Averill, Phys. Rev. Lett. **58**, 234 (1987).

[11]We call regions 1d.1, 1d.2, 2.1, and 2.2 "cones," although, in fact, they no longer formally satisfy the definition given in the Introduction, but are only derived from cones.

[12]F. W. Averill and G. S. Painter, Phys. Rev. B **32**, 2141 (1985).

[13]F. W. Averill and G. S. Painter, Phys. Rev. B **34**, 2088 (1986).

[14]G. S. Painter and F. W. Averill, Phys. Rev. B **35**, 7713 (1987).

[15]H. Anton, *Elementary Linear Algebra* (Wiley, New York, 1984).